Experimental and Theoretical Analysis of Band Formation in Polymeric Liquid Crystals upon Cessation of Flow

S. J. Picken,*,† P. Moldenaers,‡ S. Berghmans,‡ and J. Mewis‡

Akzo Research Laboratories Arnhem, Corporate Research, Physical Chemistry Department, P.O. Box 9600, 6800 SB Arnhem, The Netherlands, and Department of Chemical Engineering, Katholieke Universiteit Leuven, de Croylaan 46, B-3001 Leuven, Belgium

Received December 15, 1991; Revised Manuscript Received April 6, 1992

ABSTRACT: The evolution of the band texture, that develops in a lyotropic chiral nematic (cholesteric) PBDG solution after cessation of flow, is determined by means of a polarizing microscope equipped with a shear-flow cell. Both the real and the conoscopic SALS images are used to obtain information on the increase of the band spacing as a function of relaxation time. Also, a relation between the previously applied shear rate and the lateral band size is observed. The experimental results on the band spacing are compared to a simple one-dimensional (1-D) continuum mechanical model that uses the bend Frank elastic constant and the Miesowicz rotational viscosity. The difference between the time dependence of the lateral and the longitudinal relaxation is discussed in terms of the difference between the splay and the bend elastic constant. The spontaneous formation of a band texture during relaxation is demonstrated using a 2-D lattice model. The average "domain size" during flow as a function of shear rate is predicted using some simple scaling arguments. This prediction is compared to the experimental results.

Introduction

A long-standing observation in many main-chain polymer liquid crystals is the occurrence of the so-called band texture upon cessation of flow. It has been observed in lyotropics as well as in thermotropics. These bands have been reported for PBxG (poly(benzyl-x-glutamate), where x = L, D, or racemic) solutions in *m*-cresol,[1] for HPC ((hydroxypropyl)cellulose) solutions in water,[2-5] for PPTA (poly(*p*-phenyleneterephthalamide)) solutions[6] in H_2SO_4 and in thermotropics.[7,8] It is thus a common feature for this class of materials, although the precise details of the band formation can differ somewhat as regards the required critical preshear rate and prestrain.

The mechanism leading to the formation of band textures is still not known in detail; the concensus seems to be that the band texture is related to relaxation of the director field after cessation of flow. In this paper we propose that the anisotropy of the Frank elastic constants of the lyotropic phase (especially the splay and bend constants) provide the driving force for this phenomenon.

Here we report the results of a rheooptical study on a PBDG solution in *m*-cresol. By study of the time dependence of the real and the conoscopic SALS images, an increase of the "band spacing" can be observed. The experiments are compared to a simple one-dimensional (1-D) model. The growth of the band spacing is explained by the relaxation of a "white noise" perturbation of a fully aligned director field. Also, some results using a simple 2-D lattice model are presented. The latter can incorporate both the splay and bend elastic constants. It is used to relate the relaxation time to the characteristic "domain size" and can also provide a relatively realistic simulation of the band texture formation.

The thus obtained result for the domain size as a function of relaxation time can also be used to postulate the scaling behavior of the "domain size" during flow. This prediction is compared to some experimental results. Finally, some observations on the influence of the previously applied shear rate on the lateral and longitudinal relaxation of the band texture are reported.

Experimental Section

PBDG Sample. The rheooptical experiments were performed on a PBDG solution in *m*-cresol. The average molecular weight M_w was 310 000, and the concentration was 25% (w/w). This is about 4 times the critical concentration for the onset of liquid crystallinity in this particular system.

The steady-state rheological behavior of the sample under investigation serves as a reference for the optical studies. A Rheometrics mechanical spectrometer 705F, equipped with cone and plate geometry, has been used for this purpose. The temperature was kept at 20.0 °C. The viscosity and first normal stress difference are shown as a function of shear rate in Figure 1. The viscosity curve consists of a Newtonian region, followed by a shear thinning region. At still lower shear rates the viscosity might slightly increase again. The first normal stress difference changes from positive to negative values around a shear rate of 20.0 s^{-1}. On the basis of the data of Kiss and Porter[9] N_1 is expected to become positive again at a shear rate higher than 1000 s^{-1}.

The optical experiments presented below cover both shear rate regions with positive and negative N_1. Additional rheological data on this sample have already been reported elsewhere.[10]

Rheooptical Method.[11] The sample was sheared in a parallel plate flow cell mounted on a Leitz Orthoplan Pol polarizing microscope with crossed polars in the Hv position. Two sets of spacers were used, respectively 25 and 100 μm. A wide range of shear rates was available: respectively 0.5–500 s^{-1} for the narrow gap and 0.125–125 s^{-1} for the broader gap. The maximum strain for a complete stroke of the upper plate is respectively 300 strain units for the 25-μm sample and 75 strain units for the 100-μm sample thickness.

The images were recorded using a Panasonic WVP-F10E video camera and a Philips video recorder. Both the real and the conoscopic SALS images were recorded. The conoscopic SALS image is obtained if the incident light has a low divergence, i.e. the aperture diaphraghm is nearly closed. The conoscopic image is situated at the back focal plane of the objective lens and thus contains the directional information. Each point in the back focal plane coincides with a certain scattering **k** vector. The conoscopic SALS image provides a 2-D Fourier transform of the real image so that, for instance, a regular pattern such as the band texture will show up as a pair of meridional spots.

Steady-State Results. Visual inspection of the sample between crossed polarizers during flow was performed over two

† Akzo Research Laboratories Arnhem.
‡ Katholieke Universiteit Leuven.

0024-9297/92/2225-4759$03.00/0

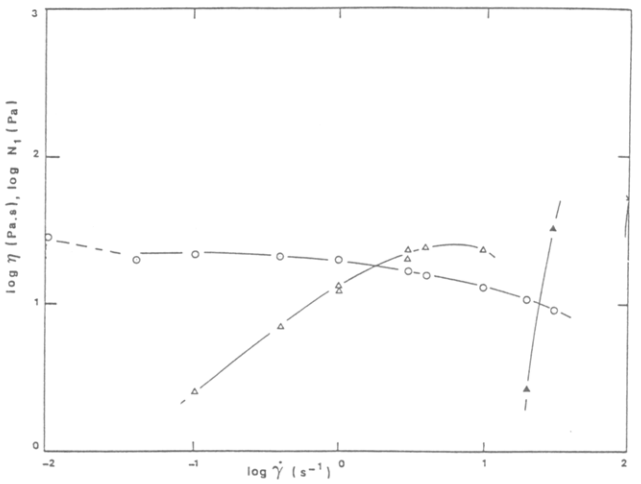

Figure 1. Steady-state viscosity (○) and first normal stress difference (△, positive; ▲, negative) as a function of shear rate for the studied PBDG sample.

decades of shear rate. At the lower shear rates (up to a few reciprocal seconds) a speckled but otherwise featureless image is recorded (see Figure 2). With increasing shear rate a striated texture develops; the striations are parallel to the shear flow direction. An example of such an image is shown in Figure 2 for a shear rate of 12.5 s^{-1} and a sample thickness of 100 μm. Further increasing the shear rate results in a refining of the structure. Near shear rates of approximately 100 s^{-1} the picture becomes progressively dark. For the thinner sample the striated texture is much less clearly visible.

Under steady-state conditions no bands perpendicular to the flow direction were observed, contrary to what was reported by Kiss and Porter.[1] This can be concluded from conoscopic images that were recorded during steady-state shearing. Typical examples are represented in Figure 3 for shear rates of 0.125, 12.5, and 62.5 s^{-1}. The image evolves from an elliptical or symmetrical crosslike structure at low shear rates to an anisotropic figure with a sharp vertical streak and diffuse lobes with increasing shear rate. Analogous images have already been obtained on other flowing liquid crystalline materials by SALS (Ernst and Navard[5] and Takebe et al.[12]) and by conoscopic SALS (Picken et al.[11]). In none of these cases were meridional reflections observed. This indicates that the band texture does not occur during flow.

Relaxation Behavior. In a first series of optical relaxation experiments the band spacing, perpendicular to the direction of flow, is measured as a function of time after the shear flow is stopped (see Figure 4 for an example). To perform this one-dimensional analysis the video image was photographed at various instances and the band spacing determined from the photographs. The spacing was defined in these experiments as the average width of a light and a dark stripe on the black and white photographs. Although it was not of specific interest to this work, the data confirmed the earlier findings that the lower the preshear rate, the longer it takes before the bands appear (Kiss and Porter[1]). A similar dependence on the preshear rate has been observed in aramid solutions ($PPTA/H_2SO_4$) using time-resolved X-ray scattering, where the degree of flow-induced orientation relaxes away more rapidly with increasing preshear rate. For the lowest shear rate that could be applied, viz. 0.125 s^{-1}, no bands were formed.

The evolution of the average thickness of the bands is shown in Figure 5 for a sample thickness of 100 μm. The previous shear rate was varied systematically between 1.25 and 125 s^{-1}. From this figure it is clear that the band thickness increases from an initial value of 10–15 μm to a value of approximately 45 μm after 100 s. Up to 10 s of rest the increase of the band thickness is rather limited and for larger times increases approximately proportional to $t^{1/2}$. Both the absolute values and the kinetics of the band growth are independent of the previous shear rate, for the two decades of shear rate under investigation.

The fact that N_1 is positive or negative during the preshear does not seem to affect the results. It could also be seen on the

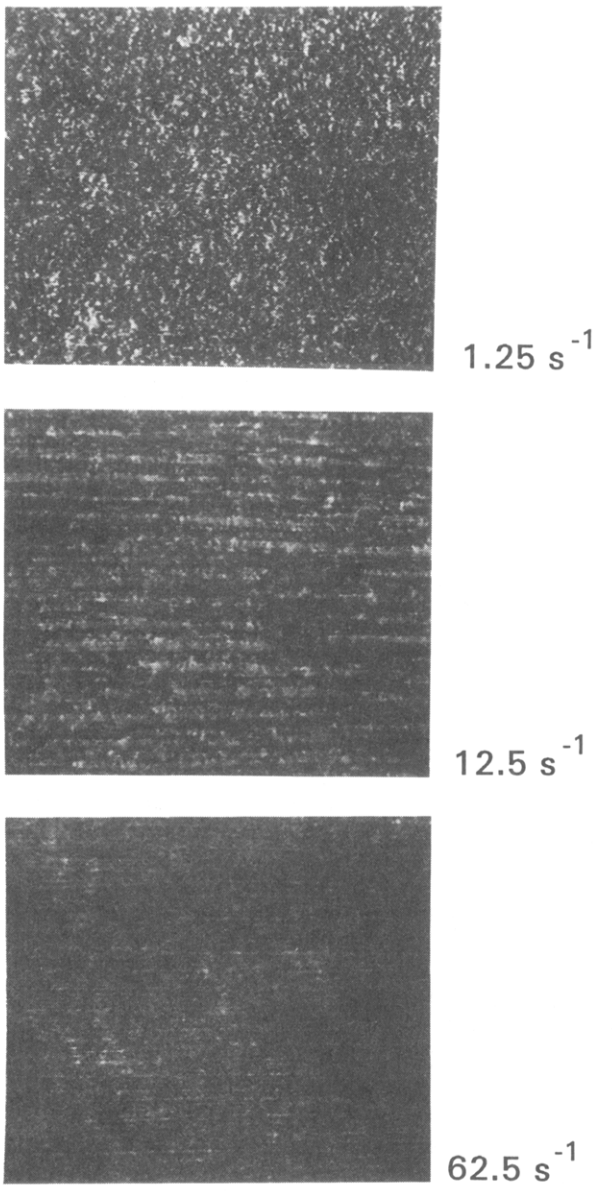

Figure 2. Patterns observed during flow using crossed polars in the Hv position at 1.25, 12.5, and 62.5 s^{-1}.

photographs that the increase of the average band thickness is due to a collapse of adjacent bands rather than to the broadening of individual bands. The latter observations has of course consequences for the mechanisms capable of explaining the phenomenon. As gap size effects can always be present in liquid crystalline materials, this effect was investigated by decreasing the gap with a factor of 4. The results for the 25-μm sample are displayed in Figure 6. Comparing Figures 5 and 6 shows that the sample thickness has little influence on the initial spacing of the bands nor their growth in time.

The kinetics of the band growth does not depend on the previous shear rate ($\dot{\gamma}_0$), unlike many slow rheological transients recorded upon cessation of flow for liquid crystals. For the particular sample under investigation the linear dynamic moduli are known to change slowly after stopping the flow. The kinetics of this evolution has been established to be inversely proportional to the previous shear rate $\dot{\gamma}_0$ (Moldenaers et al.[10]). An inverse proportionality on preshear rate has also been recorded for the tail of the stress relaxation curve of this sample. Larson and Mead[13] observed that recoil occurs over a time range which again is inversely proportional to $\dot{\gamma}_0$ for similar solutions.

An investigation of the evolution of the band spacing, using image analysis of video-recorded textures, was performed parallel with the present study on a similar solution (Gleeson et al.[14]). The image analysis technique has the advantage of avoiding

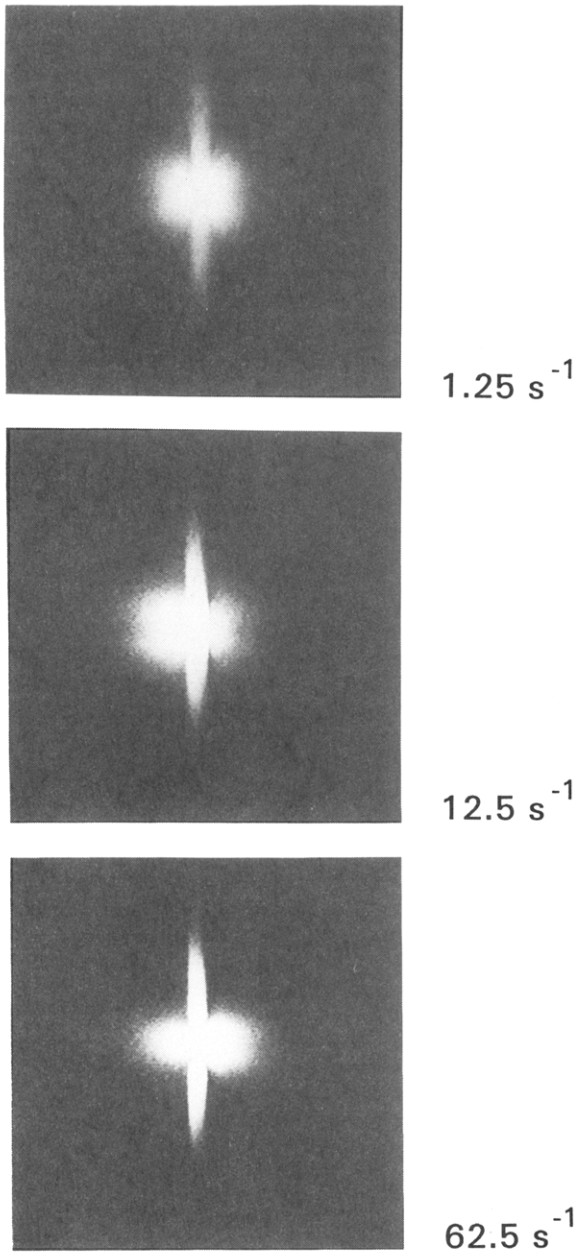

Figure 3. Conoscopic SALS images during flow for 1.25, 12.5, and 62.5 s^{-1}.

subjectivity. On the other hand, superimposed structures or irregularities will also contribute to the overall picture. The results of both studies are similar in the sense that they both report a kinetics for thickness of the bands perpendicular to the flow direction that is essentially independent of preshear rate and is not affected by the sample thickness.

Investigating the band spacing as a function of time only reveals some of the phenomena that are going on after cessation of the shear flow. It is obvious from the series of pictures (Figure 4) that not only the spacing but also the lateral dimension of the bands evolves with time. Measuring this (average) lateral length, as such, was not easy to do. In order to quantify the lateral direction, the number of "connected white regions" (the individual bands) per arbitrary surface area was determined as a function of time. The thus obtained number of bands for the sample with a thickness of 100 μm is shown in Figure 7 for the same preshear rates as reported in Figure 5. The inverse of the number of bands yields a measure for the average area of a band in the shear-neutral plane. It is obvious from Figure 7 that the change of the average surface depends on $\dot{\gamma}_0$. The higher the previous shear rate, the faster the number of bands decreases as a function of time. It was, however, reported above that the evolution of the thickness of the bands was shear rate independent. Consequently, the shear rate effect reported here must be attributed to an increase of the lateral band size in the direction perpendicular to that of the flow. This increase in lateral band size by and large takes place before the thickness of the bands substantially increases. If there was no difference in growth speed, no band formation would be observed. Bearing in mind the often encountered inverse proportionality on $\dot{\gamma}_0$ for many rheological transients, the data of Figure 7 were replotted in Figure 8 versus rest time multiplied by the previous shear rate. From Figure 8 it can be concluded that the curves for the seven shear rates superimpose well when scaled in this manner.

Simple Continuum Mechanical Theory for the Band Spacing

The initial texture after cessation of flow seems to be related to elastic recoil of the sample, indeed back-flow can be observed after the shear flow has been stopped. Simultaneously, a dramatic increase in depolarization is observed. This means that the elastically stored energy during flow is dissipated, apparently leading to instabilities in the director alignment. A similar phenomenon is observed in 20% (w/w) PPTA/H_2SO_4 solutions.[11]

The elastic storage in a nematic phase is either in the molecules themselves and/or in the macroscopic texture of the nematic phase. A mechanism for the storage of elastic energy in the texture of the liquid crystal has been proposed in terms of an affine deformation of a "disclination gas" type texture.[11] In this model the elongational component of the applied strain leads to a stretching of the disclination gas and thus to an increase of the Frank elastic energy stored in the continuum surrounding the defect structure. This explains the observation of a recoverable strain as high as 15 units in nonequilibrium recoil experiments.[11] We find it hard to envisage a reasonable molecular mechanism to explain this phenomenon. Although interesting, we will not study the recoil and director instability phenomenon further. Instead we will use the flow-induced instabilities as a starting point for calculating the relaxation behavior. To avoid any misunderstanding, the perturbation of the director upon cessation of flow that we envisage is entirely due to flow instabilities and should not be confused with thermal fluctuations of the director field. We also note that compared to low molecular weight nematics the thermal director fluctuations are not visible, or at least we have never seen any. This is presumably due to the much higher viscosities in polymeric materials.

Here a simple continuum mechanical model will be described that allows the calculation of the band texture. The idea is that, upon cessation of flow, a "random" perturbation of the oriented director field occurs (of as yet unspecified origin). The relaxation of this perturbation is driven by the Frank elastic constants K_i and dissipated by the Miesowicz rotational viscosity γ_1.

The Frank elastic energy is given by[15,16]

$$F_{el} = \frac{1}{2}(K_1(\text{div } n)^2 + K_2(n\cdot\text{curl } n)^2 + K_3(n \times \text{curl } n)^2) \quad (1)$$

For the first calculation we now will assume perfect lateral order and will start with a white noise perturbation of the director field orientation angle along the direction of flow (see Figure 9). Here we will assume that the perturbation is small, i.e. much less than $\pm\pi/4$ radians. This effectively is a 1-D description of the problem, where we only focus on the band spacing as a function of time. In this special case only bend modes are possible; i.e. we only use K_3 for the time being. Due to the white noise pertubation, initially all spatial frequencies k along the direction of flow are equally probable. During relaxation this k

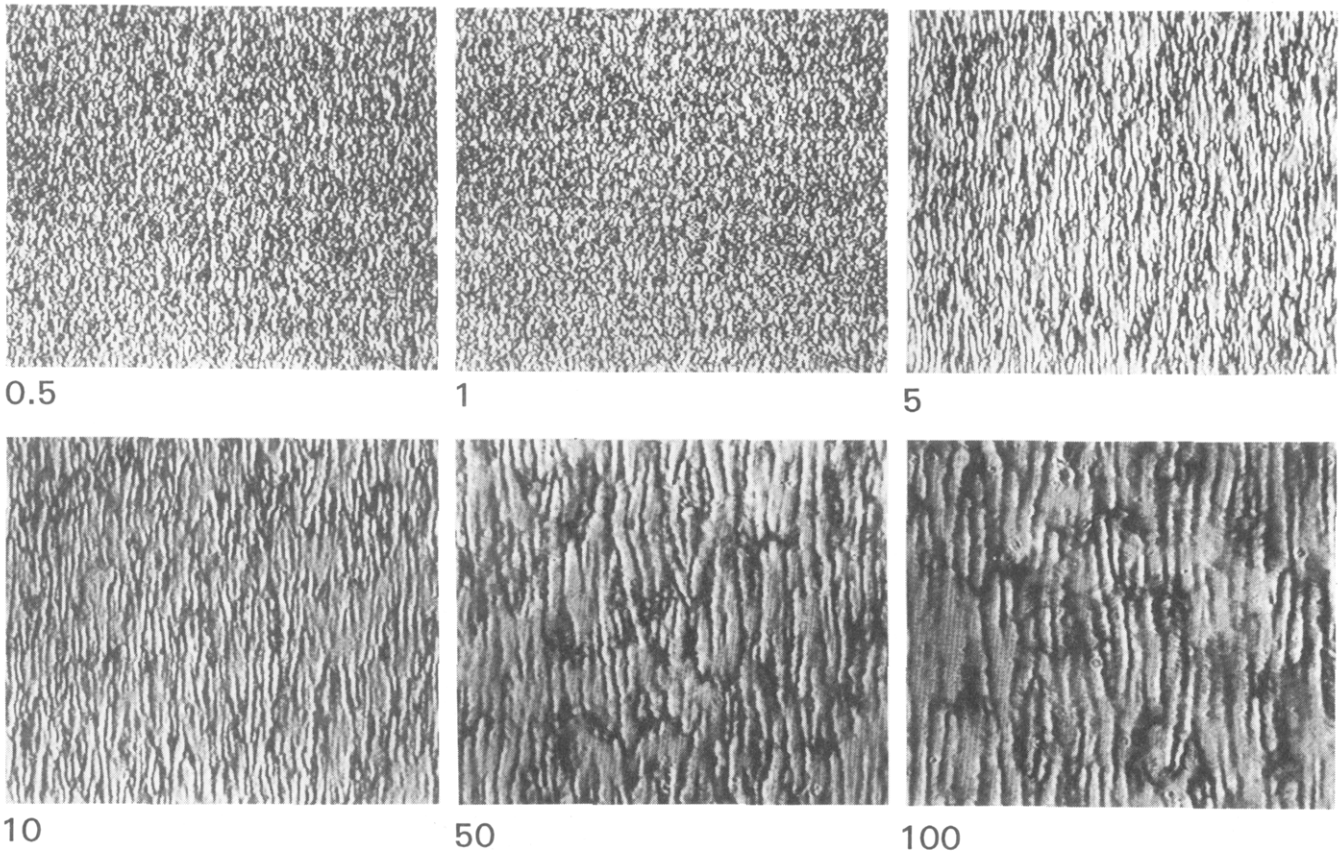

Figure 4. Time dependence for the band texture after cessation of flow: preshear rate, 12.5 s^{-1}; thickness, 100 μm; real images. The indicated times are in seconds.

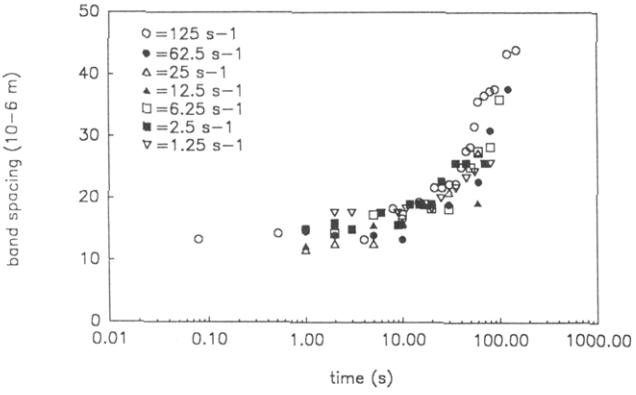

Figure 5. Band spacing as a function of time for the 100-μm sample.

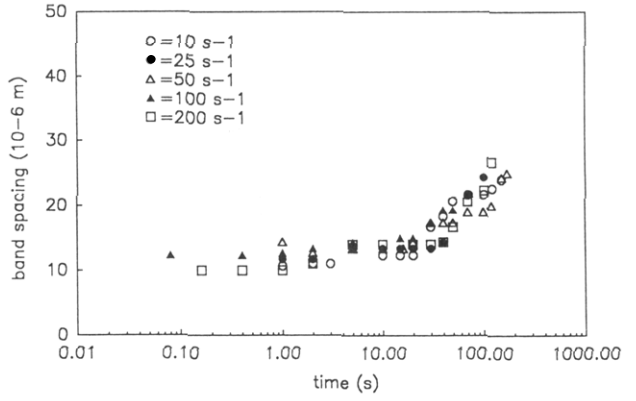

Figure 6. Band spacing as a function of time for the 25-μm sample.

spectrum changes. Due to the higher curvature the highest spatial frequencies disappear more rapidly than the lower ones. Consequently, a characteristic length scale for the band texture will appear.

The differential equation describing the relaxation of the perturbed director field is given for small deviations by[16]

$$\gamma_1 \frac{d\varphi}{dt} = K_3 \frac{d^2\varphi}{dz^2} \tag{2}$$

Where $\varphi(z,t)$ is the time-dependent deviation angle of the director orientation along the direction of flow z. Separation of variables leads to the general solution

$$\varphi(z,t) = (2\pi)^{-1} \int_{-\infty}^{\infty} dk\ \varphi(k,0)\ e^{ikz} \exp(-K_3 k^2 t/\gamma_1) \tag{3}$$

Where $\varphi(k,0)$ is the Fourier transform of $\varphi(z,0)$. From eq 3 it is observed that indeed the high-k part of the deviation decays most rapidly (see Figure 9). The characteristic length scale for the decay process is in the order of $2\pi/k$ thus

$$L \simeq 2\pi(K_3 t/\gamma_1)^{1/2} \tag{4}$$

In the present work L is assumed to be proportional to (and in the order of) the band spacing. This could have been derived immediately from eq 2 using scaling analysis. An identical equation has been used by Larson and Mead[13] to describe the evolution of the domain size after cessation of flow. Finally, it is perhaps useful to note that the process we describe is similar to an effect known from acoustics. If white noise is passed through a simple low-pass filter the result is "pink noise" which has a definate pitch that is related to the cutoff frequency of the filter.

To illustrate these equations, a simple Turbo-Pascal (Borland) program was written to simulate the appearance of a band texture as a function of time. In Figures 9 and 10 we show the random initial perturbation of the director angle and its time dependence. The exponent for L versus

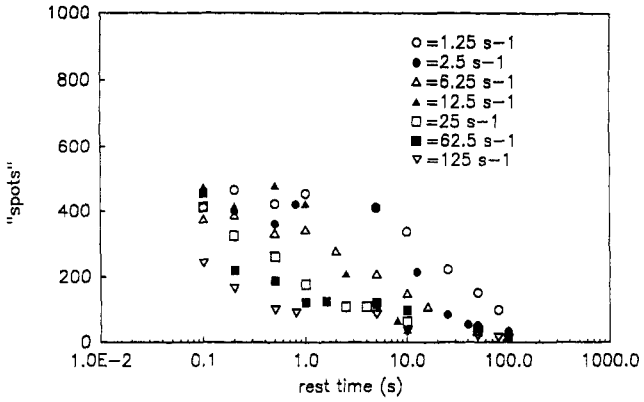

Figure 7. Number of connected white regions as a function of relaxation time, for various shear rates as indicated (100-μm sample).

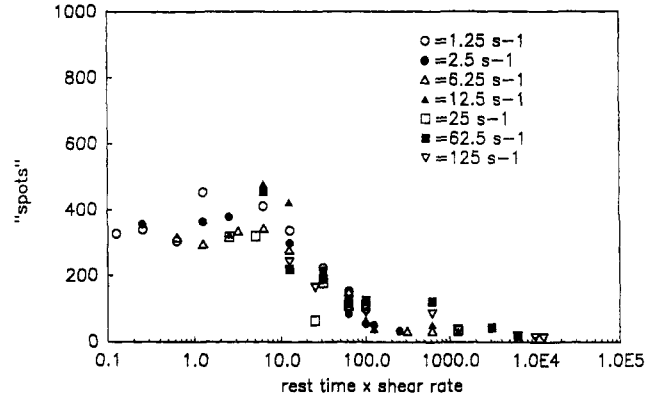

Figure 8. Number of connected white regions as a function of relaxation time multiplied by the applied preshear rate. Shear rates are as indicated.

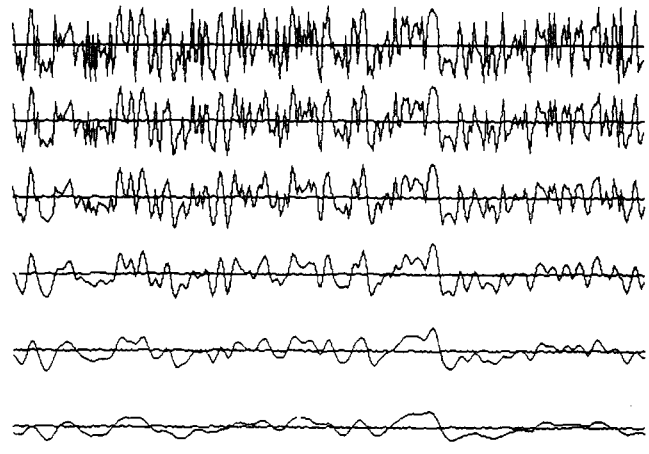

Figure 9. Initial white noise perturbation of the director field orientation angle $\varphi(z,0)$ and evolution $\varphi(z,t)$ after various periods of rest (eq 3), where the domain size L is respectively 0, 0.67, 1.1, 1.8, 3, and 5% of the shown interval.

t of 1/2, from eq 4, is in reasonable agreement with the large t behavior for the band spacing that we found experimentally.

Instead of considering the real images it is also instructive to analyze the decay of the k spectrum in reciprocal space. In Figure 11 we show a white noise spectrum at $t = 0$ and the corresponding spectrum for various scaled relaxation times K_3t/γ_1. From eq 3 it is observed that the spectrum decays as $\exp[-(K_3t/\gamma_1)k^2]$, which is just a Gaussian function of k.

The one-dimensional image analysis data reported by Gleeson et al.[14] seems to be comparable with the one-dimensional model presented here. They both indicate

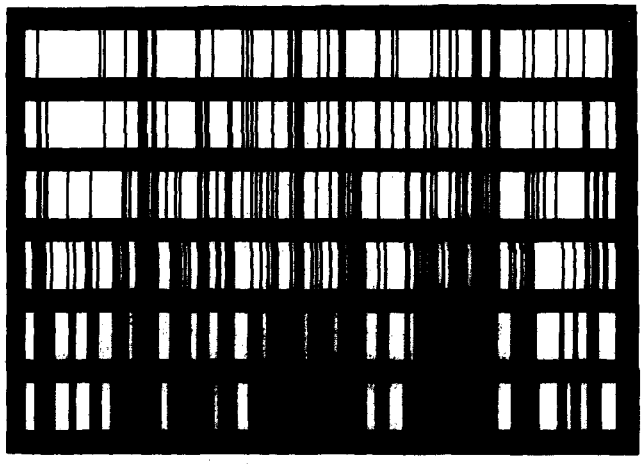

Figure 10. Appearance of a band texture as a function of time using the 1-D model, eq 3. Domain sizes are as in Figure 9.

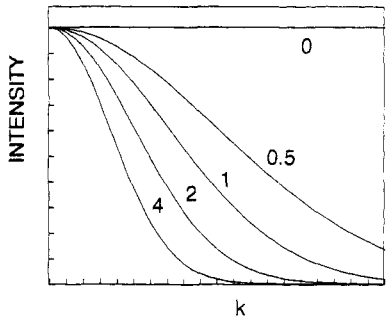

Figure 11. Spatial frequency (k) spectrum as a function of rest time (arbitrary units).

the prime importance of considering a spectrum of spatial frequencies in the band texture problem. It is noted that a single spatial frequency k perturbation (i.e. a sine wave) cannot change its characteristic length scale as function of time; only the intensity of the deviation will decrease. The use of a spectrum of k values is required to explain the occurrence of bands that (appear to) grow apart as a function of time.

Of course it is not strictly necessary to start with a white k spectrum and indeed one may speculate that the highest spatial frequency that occurs is in some way related to the preshear rate. By using eq 2 together with the general rule that the application of a simple shear flow with rate $\dot{\gamma}$ will only affect processes with a relaxation time greater than or equal to $1/\dot{\gamma}$, it is immediately derived that, during flow, we may expect the following for the domain size L':

$$L' \simeq 2\pi(K_3/\gamma_1\dot{\gamma})^{1/2} \tag{5}$$

that is with increasing shear rate the optical texture should become more finely structured.[17] This trend is observed experimentally for the domain size (see Figure 2). The correspondence between time and shear rate effects has been confirmed in rheological experiments.[10] However, the exponent $\dot{\gamma}^{-1/2}$ was not seen in the present experiments as can be observed from Figure 2 where the domain size during flow seems to depend only slightly on the applied shear rate (at least for 1.25 and 12.5 s^{-1}).

Of course the high wavenumber cutoff of the power spectrum during flow should not influence the long time relaxation behavior of the band texture. This means that using our model the preshear rate should not influence the ultimate band texture. This is true for the band spacing (see Figures 5 and 6); however, it is not true for the lateral band dimension as indicated by the number of spots being a function of the dimensionless rest time (see Figure 8).

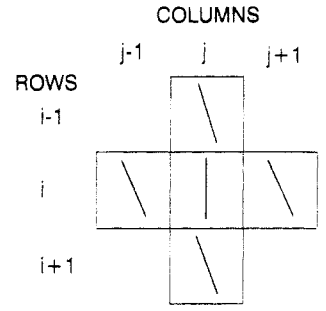

Figure 12. Example of the surrounding of cell i, j. Here the cells $i, j-1$ and $i, j+1$ contribute a splay energy to $(F_{el})_{ij}$ and the $i-1, j$ and $i+1, j$ cells contribute bend energy.

In the following section on the 2-D model we will return to this point.

As regards the minimum shear rate required for band formation (between 0.125 and 0.25 s^{-1} for the 100-μm sample), this is not in disagreement with the present model. If we assume that due to random boundary conditions the samples are not uniformly aligned at rest, then there will be a minimum shear rate required to align the director. This may be compared to a Fredericks transition where the surface anchoring of a sample is only overcome by an external magnetic field above a certain critical value. The band texture is then only found if a shear rate above the critical value is applied. Note that in this approach the critical shear rate should depend on the gap.

We did not observe an influence of the gap spacing on the critical shear rate; however the minimum shear rate that could be applied on the 25-μm sample was 4 times higher than that for the 100-μm sample. This means that the low shear regime could not be studied for the thinner sample. The question arises if the characteristic length scale, determining the critical shear rate, is the gap spacing itself or a "characteristic domain size" in the sample. In the latter case the critical shear rate would be independent of the gap unless the gap spacing is less than the characteristic domain size.

2-D Lattice Model for Lateral and Longitudinal Relaxation

To study the relaxation behavior further, a more general 2-D lattice model has been used. This provides the possibiliy to calculate the texture from a given initial director field. A similar approach has been used before by Bedford et al.[18,19] to show the growth of nematic domains. Here we will use a simple 2-D lattice where only splay and bend deformations can occur. It is noted that for small perturbations of the director field the longitudinal relaxation will be mainly determined by the bend elastic constant K_3, as used before, and that the lateral relaxation is driven by the splay modulus K_1. From the more rapid lateral relaxation observed experimentally it may immediately be concluded that $K_1 > K_3$. Now the Frank free energy will be approximated for each cell ij of the discrete 2-D lattice:

$$(F_{el})_{ij} = \sum_{kl} \frac{1}{2}(K_1 \sin^2(\alpha_{ijkl}) + K_3 \cos^2(\alpha_{ijkl})) \sin^2(\varphi_{kl} - \varphi_{ij}) \quad (6)$$

Where the kl summation is over the four nearest neighbor cells of cell ij and where the angle α_{ijkl} is the angle between the vector $\mathbf{r}_{ij} - \mathbf{r}_{kl}$ and φ_{ij}. The angle α_{ijkl} determines to what extent a splay or a bend mode is contributing to the elastic free energy of the cell (see Figure 12).

Explicitly differentiating this expression with respect to the director orientation angle φ_{ij}, we obtain the torque due to the Frank elasticity on cell ij:

$$M_{ij} = \sum_{kl} -\frac{1}{2}(K_1 \sin^2(\alpha_{ijkl}) + K_3 \cos^2(\alpha_{ijkl})) \sin(2(\varphi_{kl} - \varphi_{ij})) \quad (7)$$

This can be simplified for computational purposes by substituting $K_1 = 2Kr$ and $K_3 = 2K(1 - r)$ so that K determines the average value of the elastic contants and r provides a sliding scale between only bend ($r = 0$) and only splay ($r = 1$) elasticity:

$$M_{ij} = \sum_{kl} -K(r \sin^2(\alpha_{ijkl}) + (1 - r) \cos^2(\alpha_{ijkl})) \sin(2(\varphi_{kl} - \varphi_{ij})) \quad (8)$$

The one-constant approach ($K_1 = K_3$) can be obtained by setting $r = 1/2$.

Using the differential equation for $\varphi(z,t)$ and taking discrete time steps, we obtain the iterative equation for the 2-D lattice model:

$$\varphi_{ij}(t + \Delta t) := \varphi_{ij}(t) + CM_{ij}/K \quad (9)$$

where C determines the rate of convergence of the algorithm. Each iteration corresponds to a single time step $\Delta t = C\gamma_1/K$. As always to obtain satisfactory convergence of the algorithm the rate constant C has to be chosen sufficiently small.

Now two examples of the lattice model results will be presented. First, a completely random lattice is used as a starting point (see Figure 13). The boundaries of the lattice are not iterated so that random boundary conditions are applied throughout the simulation. The small circles in the figure show the large number of +1/2 and −1/2 disclinations in the initial structure. These are detected by calculating the cumulative angle difference when closed loops around the corners (nodes) of four adjacent cells are traversed.

As a function of "time" or iteration number the texture becomes more homogenous leading to a reduction in the number of disclinations (see Figure 13). Here for simplicity we use equal values for the splay and the bend elastic constants, i.e. $r = 1/2$ in eq 8. It is observed that the director field becomes more homogeneous by mutual annihilation of disclinations of unlike sign. The disclinations effectively act as "charged particles" of +1/2 and −1/2 charge. When the number of disclinations is counted as a function of time the domain size L_d, given by $L_d = (1/N)^{1/2}$ i.e. the square root of the average surface per disclination, can be calculated. In Figure 14 the log of this domain size is shown as a function of log t. The slope is found to be 0.5, i.e. a length (the size) scales as $t^{1/2}$ in agreement with the scaling analysis presented before.

One slightly disturbing result of the lattice model is the absence of +1 and −1 disclinations that are often found in real nematic liquid crystals. As such the Frank energy involved with these disclinations is 4 times higher than for the half-integer disclinations so that this result is not surprising for the 2-D simulation. Nevertheless the discrepancy with experimental results is not entirely pleasing. It has been suggested[20,21] that the elastic energy of integer disclinations can be reduced in 3-D systems via an out of plane distortion: the escape in the third dimension. The procedure that detects the disclinations in our 2-D simulations only uses the four adjacent cells of a node, which excludes the possibility to detect integer disclinations anyway. To improve matters, a triangular lattice

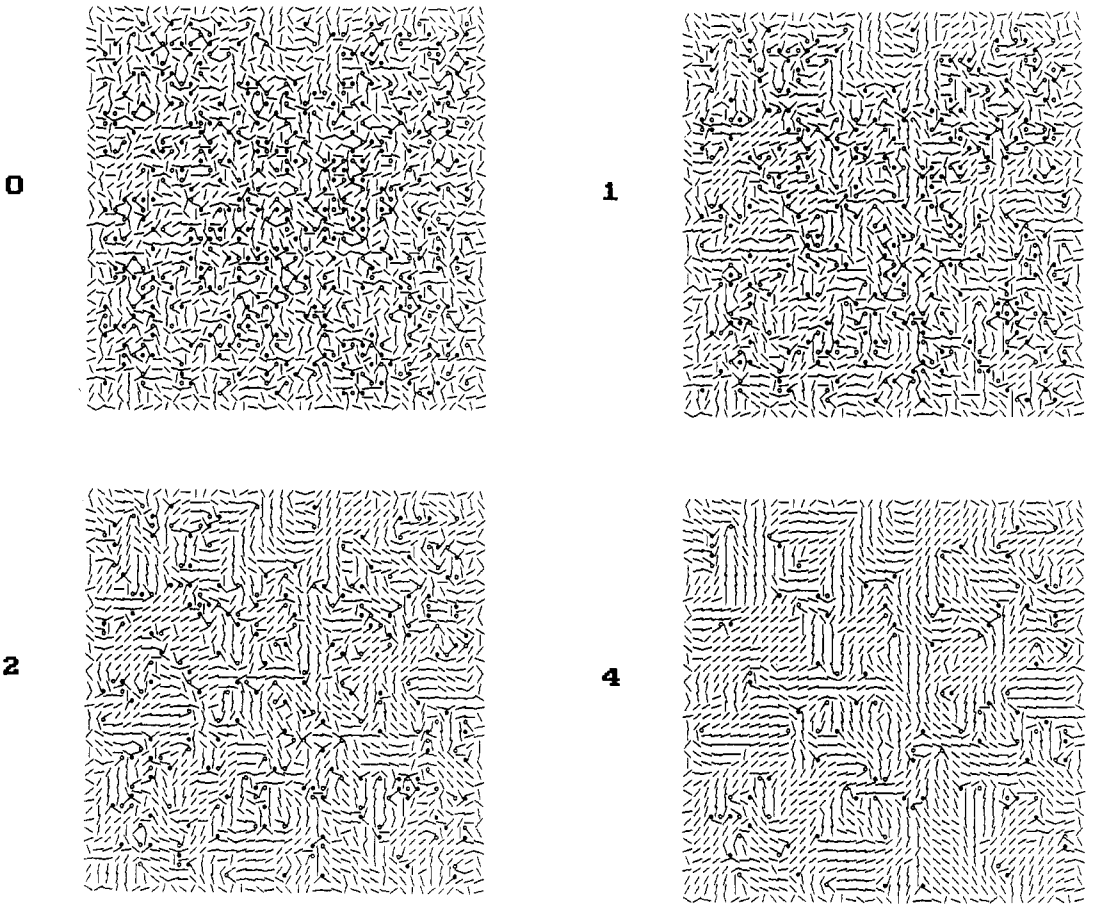

Figure 13. Relaxation of a completely random initial texture, using the 2-D model, with $r = 1/2$ (one constant approach). The drawn circles are the disclinations. The iteration count indicates the number of time steps.

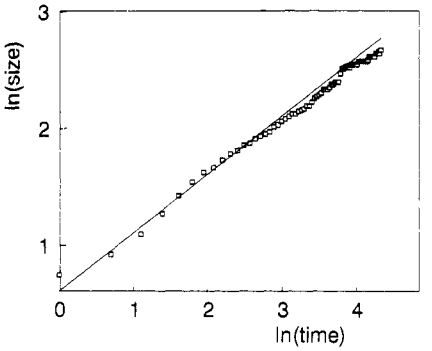

Figure 14. Domain size, or the square root of the reciprocal number of disclinations per unit area, as a function of time on a log–log scale.

could be used instead with six adjacent cells per node. In addition 3-D lattice simulations might be instructive to clarify matters further.

As a second example the relaxation of a randomly perturbed uniform director field will be shown. The relaxation behavior can now be studied as a function of time in two dimensions. The white noise perturbations as before are assumed to be due to the cessation of flow (see Figure 15). The perturbation angle for each cell was chosen at random between +1 and −1 radians. For the elastic constants we use $r = 0.99$, i.e. $K_1/K_3 = 99$. The choice of this ratio is for demonstration purposes only. It is well-known that the splay constant is larger than the bend constant in these systems (as has been discussed by Meyer[22,23] and Odijk[24]) and is thought to be due to the fact that a splay deformation leads to the creation of "free volume" that has to be filled up by reptation of chain ends and/or hairpins. The ratio of the elastic constants for PBDG could in principle be estimated from the model presented by Odijk.[24] In Figure 15 the results of the lattice model are shown. For clarity only the cells with orientations that deviate from uniform planar alignment are shown.

From Figure 15 it is observed that the lateral correlation length increases more rapidly than the longitudinal one leading to a "band texture". For the ratio of the elastic constants chosen in the simulation the lateral correlation length is about 10 ($\approx\sqrt{99}$) times larger than the longitudinal correlation length. From the time dependence of the lateral and longitudinal correlation length, respectively given by $L_\perp = 2\pi(K_1 t/\gamma_1)^{1/2}$ and $L_\parallel = 2\pi(K_3 t/\gamma_1)^{1/2}$, the ratio is given by $L_\perp/L_\parallel = (K_1/K_3)^{1/2}$. From the experimentally measured band textures we estimate $L_\perp/L_\parallel \simeq 5$–10 so that from the experiments we expect $K_1/K_3 \simeq 25$ – 100.

This ratio is in reasonable agreement with the ratios reported by Hakemi,[25] i.e. $K_1/K_3 = 100$. However, it is much higher than the ratios reported by Lee and Meyer,[26] around about 0.7–1.2, admittedly for lower polymer concentrations. We note that the results of Hakemi[25] indicate a large influence of M_w on the K_1/K_3 ratio; this is not confirmed by the results of Lee and Meyer[26] at lower concentrations. It is perhaps reasonable to assume that with increasing polymer concentration the ratio K_1/K_3 will increase due to the higher degree of molecular orientation. However, the large difference with the splay-bend ratios reported by Lee and Meyer[26] is still somewhat worrying.

From the analysis presented above it is clear that from the present model the aspect ratio of the bands $L_\perp/L_\parallel$ is expected to be constant (and equal to $(K_1/K_3)^{1/2}$). This is not in agreement with the experimental results where

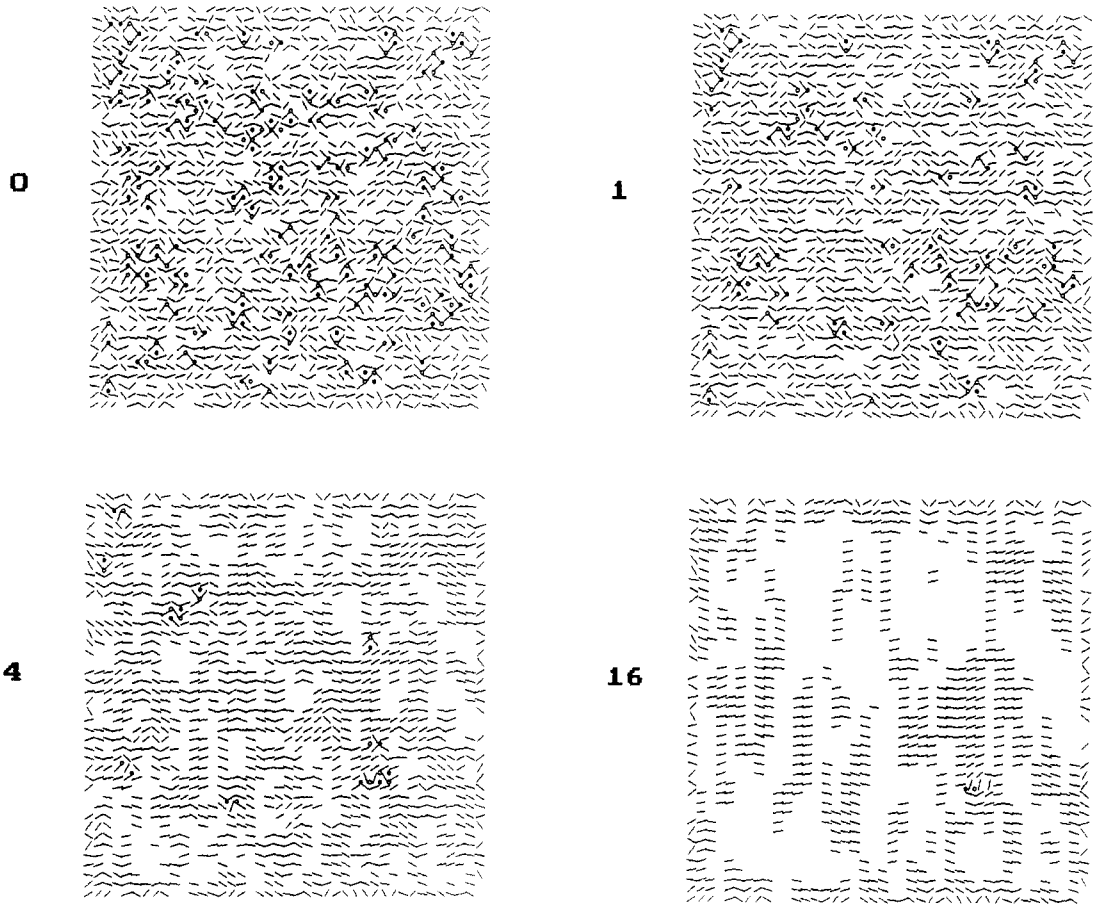

Figure 15. Relaxation of a randomly perturbed planar texture, using the 2-D model, with $r = 0.99$ (i.e. $K_1/K_3 = 99$). The drawn circles are the disclinations. The iteration count indicates the rest period (number of time steps). Note the rapid increase of the degree of lateral correlation. The cells oriented parallel or perpendicular to the "polars" are not printed for clarity.

the lateral correlation length seems to depend on the applied preshear rate. Possibly, the applied preshear rate influences the details of the initial texture that is formed upon cessation of flow. As regards the relaxation of the "number of spots" (Figures 7 and 8), if we assume the number of spots N_s to be proportional to $1/(L_\perp L_\parallel)$, then using our model we derive that

$$N_s \sim \frac{1}{L_\perp L_\parallel} = \frac{\gamma_1}{4\pi^2 (K_1 K_3)^{1/2} t} \tag{10}$$

This is in reasonable agreement with the shape of the decay curve shown in Figure 8, for $\dot{\gamma}t \geq 10$. The effect of $\dot{\gamma}$ on $L_\parallel$ still requires further study.

Discussion

From the experimental results that we present and the models that we propose, we conclude that the band texture phenomenon can be adequately explained by director relaxation. The rapid lateral relaxation is attributed to the large value of the splay constant in polymeric liquid crystals. This explains why the band texture phenomenon is not observed in low molecular weight nematics: the splay/twist ratio K_1/K_3 is too small. To obtain a band texture using our approach, it is sufficient to assume a spectrum of director fluctuations upon cessation of flow and a relatively large splay/bend ratio. The main disturbing feature of our model is the required high splay/bend ratio, which is not in agreement with some of the available literature.[26] It is hoped that in future experiments this can be clarified. A possibility would be to systematically vary the polymer concentration and/or average molecular weight, thereby exploring a range of K_1/K_3 ratios. Note that using our model a parallel band formation process should be observed in materials with long rigid rod particles (where the K_1/K_3 ratio might be reversed compared to the present wormlike particles).

In the present model we do not propose a detailed explanation for the required director instabilities upon cessation of flow; however, we believe them to be related to elastic storage phenomena, another property characteristic for polymer liquid crystals. Of course, it is still necessary to perform a more detailed analysis of the recoil phenomenon and to study the precise details of the deformation spectrum upon cessation of flow. This would perhaps allow explanation of the influence of the preshear rate on the lateral band size. In addition, it would be worthwhile to perform a complete 3-D simulation of the director relaxation. Nevertheless, we do not expect such refinements to seriously alter the general arguments for the formation of the band texture that we present here.

Acknowledgment. The work performed at the University of Leuven was made possible due to the financial support of Akzo. We thank Prof. D. Frenkel for some critical remarks and some suggestion for further improvement of the lattice model.

References and Notes

(1) Kiss, G.; Porter, R. *Mol. Cryst. Liq. Cryst.* **1980**, *60*, 267–280.
(2) Marsano, E.; Carpaneto, L.; Ciferri, A. *Mol. Cryst. Liq. Cryst.* **1988**, *158*, 267–278.
(3) Fried, F.; Sixou, P. *Mol. Cryst. Liq. Cryst.* **1988**, *158B*, 163.
(4) Fincher, C. R. *Mol. Cryst. Liq. Cryst.* **1988**, *155*, 559–570.
(5) Ernst, B.; Navard, P. *Macromolecules* **1989**, *22*, 1419–1422.

(6) Horio, M.; Ishikawa, S.; Oda, K. *J. Appl. Polym. Sci., Appl. Polym. Symp.* **1985**, *41*, 269.
(7) Donald, A. M.; Viney, C.; Windle, A. H. *Polymer* **1983**, *24*, 155–159.
(8) Grazziano, P. J.; Mackley, M. R. *Mol. Cryst. Liq. Cryst.* **1984**, *106*, 73–93.
(9) Kiss, G.; Porter, R. S. *J. Polym. Sci., Polym. Symp.* **1978**, *65*, 193.
(10) Moldenaers, P.; Yanase, H.; Mewis, J. In *Liquid Crystalline Polymers*; ACS Symposium series 435; American Chemical Society: Washington, DC, 1990; pp 370–380.
(11) Picken, S. J.; Aerts, J.; Doppert, H. L.; Reuvers, A. J.; Northolt, M. G. *Macromolecules* **1991**, *24*, 1366.
(12) Takabe, T.; Hashimoto, T.; Ernst, B.; Navard, P.; Stein, R. S. *J. Chem. Phys.* **1990**, *92*, 1386–1396.
(13) Larson, R. G.; Mead, D. W. *J. Rheol.* **1989**, *33*, 1251–1281.
(14) Gleeson, J. T.; Larson, R. G.; Mead, D. W.; Kiss, G.; Cladis, P. E. *Liq. Cryst.* **1992**, *11*, 341-364.
(15) Frank, F. C. *Discuss. Faraday Soc.* **1958**, *25*, 19.
(16) Vertogen, G.; de Jeu, W. H. *Thermotropic Liquid Crystals: Fundamentals*; Spinger Verlag: Berlin, 1988.
(17) Marrucci, G. *Pure Appl. Chem.* **1985**, *57*, 1545.
(18) Bedford, S. E.; Nicholson, T. M.; Windle, A. H. *Liq. Cryst.* **1991**, *10*, 63.
(19) Bedford, S. E.; Windle, A. H. Poster at the Polymer Physics conference, Bristol, April 3–5, 1991.
(20) Meyer, R. B. *Philos. Mag.* **1972**, *33*, 591.
(21) Cladis, P. E.; Kléman, M. *J. Phys.* **1972**, *33*, 591.
(22) Meyer, R. B. In *Polymer Liquid Crystals*; Ciferri, A., Krigbaum, W. R., Meyer, R. B., Eds.; Academic: New York, 1982.
(23) Taratuta, V. G.; Lonberg, F.; Meyer, R. B. *Phys. Rev. A* **1988**, *37*, 1831.
(24) Odijk, T. *Liq. Cryst.* **1986**, *1*, 553.
(25) Hakemi, H. *Mol. Cryst. Liq. Cryst.* **1987**, *153*, 99.
(26) Lee, S.-D.; Meyer, R. B. *Phys. Rev. Lett.* **1988**, *61*, 2217.